



HAL
open science

On the origin of the Hall–Petch law: A 3D-dislocation dynamics simulation investigation

Maoyuan Jiang, Ghiath Monnet, Benoit Devincre

► To cite this version:

Maoyuan Jiang, Ghiath Monnet, Benoit Devincre. On the origin of the Hall–Petch law: A 3D-dislocation dynamics simulation investigation. *Acta Materialia*, 2021, 209, pp.116783. 10.1016/j.actamat.2021.116783 . hal-03260921

HAL Id: hal-03260921

<https://hal.science/hal-03260921>

Submitted on 24 Apr 2023

HAL is a multi-disciplinary open access archive for the deposit and dissemination of scientific research documents, whether they are published or not. The documents may come from teaching and research institutions in France or abroad, or from public or private research centers.

L'archive ouverte pluridisciplinaire **HAL**, est destinée au dépôt et à la diffusion de documents scientifiques de niveau recherche, publiés ou non, émanant des établissements d'enseignement et de recherche français ou étrangers, des laboratoires publics ou privés.



Distributed under a Creative Commons Attribution - NonCommercial 4.0 International License

On the origin of the Hall-Petch law: a 3D-Dislocation Dynamics simulation investigation

Maoyuan Jiang^{a,b,*}, Ghiath Monnet^b, Benoit Devincre^a

^a CNRS - ONERA, LEM, 29 Avenue de la Division Leclerc, 92322 Chatillon Cedex, France

^b EDF-R&D, MMC, Avenues des Renardières, 77680, Moret sur Loing, France

Abstract

3D-DD simulations are performed with cubic grains ranging from 1 to 10 μm to investigate the physical mechanisms at the origin of the Hall-Petch law. In particular, the long-range stress (back stress) induced by the density of polarized dislocations (GNDs) accumulated at GBs is quantified separately from the short-range stress associated with the forest dislocation (SSDs) density. We show that the back stress and the associated strain hardening is independent of grain size at low strain. Hence, the grain size effect reproduced by 3D-DD simulations is controlled by an increase of the CRSS when decreasing grain size. Such evolution of the CRSS amplitude is controlled by two competing strengthening mechanisms justifying the generic $1/\sqrt{d}$ dependent form of the Hall-Petch law observed in simulations and experiments.

Keywords: DD simulations, Hall-Petch effect, GNDs density, Crystal plasticity

1. Introduction

In a seminal works, Hall and Petch [1, 2] demonstrated for the first time the existence of a grain size effect on mechanical properties in mild steels. From these works and the many following investigations, an empirical relationship was established between yield stress σ_y and grain size d , known as the Hall-Petch

*Corresponding author.

Email address: maoyuan.jiang@gmail.com (Maoyuan Jiang)

(HP) law:

$$\sigma_y = \sigma_0 + K \frac{1}{\sqrt{d}} \quad (1)$$

where σ_0 is a reference stress generally called friction stress and K is a material constant called the HP constant. Armstrong *et al.* [3] provided later evidence that the HP law is equally applicable to the entire stress-strain curve for most polycrystalline materials. Since then, much work has been made to validate the existence of the HP law in a wide range of metals and alloys [4–6].

However, the exact form of the HP law (Eq. 1), as well as its origin are still under discussion. For example, the question of a variation of the HP constant K with plastic deformation is a matter of many debates. Some claim that K increases [7] with plastic deformation, while others suggest that K is invariant or decreases slightly with plastic deformation, as cited in [8, 9]. Other discussions focus on the mathematical form that gives the most general fit of the experimental data and several alternative forms to Eq. 1 have been proposed [10–13]. Moreover, although the “*smaller is stronger*” effect is experimentally confirmed in many polycrystalline materials with submicron and micron grain sizes, the main basic mechanism controlling this effect is still not clearly identified. In a recent review, Cordero *et al.* [7] re-examined many existing models in a systematic way by considering the numerous experimental studies published over the last six decades on pure metals. Their conclusion is that the strain-hardening model proposed by Ashby for grain size strengthening [14] is the most consistent with existing data. On the other hand, recent studies based on statistic approaches applied to a large experimental data set have shown that the effect of grain size may not evolve as $1/\sqrt{d}$, but rather follow more consistent trends with $1/d$ or $\ln(d)/d$ [15–17]. This suggests that the HP effect could be controlled by dislocation line tension effects associated to specific elements of the dislocation microstructure. As a consequence, the HP constant K might rather be insensitive to plastic deformation and highly depend on the size of grains.

Several types of simulation have been used to investigate the HP effect. These simulations provide a detailed description of the dislocation microstruc-

tures and a calculation of the interaction force between dislocations and various obstacles, such as forest segments, precipitates, grain boundaries, etc. Through molecular dynamics simulations, we know that grain boundaries (GB) are important obstacles to the free expansion of dislocations and are therefore a key component of strain hardening [18–21]. In order to study plastic deformation in the micrometer range, discrete dislocation dynamics is a very efficient method. 2D dislocation dynamics (DD) simulations [22–26] reproduce a grain size effect, but cannot provide definitive answers because important dislocation properties, such as cross-slip and line tension are ignored or oversimplified. To quantitatively unravel the plastic properties of polycrystals, 3D-DD simulations are a solution. For example, Ohashi *et al.* [27] have shown that the increase of yield stress observed in small grains is related to a shortening of dislocation sources. De Sansal *et al.* [28] studied the HP effect in periodic polycrystalline aggregates composed of regular polyhedral grains and obtained an HP exponent n between $-1/2$ and -1 . Zhou and LeSar [29] studied the size-dependent plasticity of free-standing polycrystalline thin films and developed a strengthening model based on the length of spiral sources. Yellakara and Wang [30] studied the response of polycrystalline thin films and reported a variation of the HP exponent with the shape of the simulated grains. Zhang *et al.* [31] calculated the storage rate of geometrically necessary dislocations (GNDs) at GBs and incorporated this quantity into a strain-gradient crystal plasticity model. Fan *et al.* [32] have shown that the grain size effect in ultrafine-grained magnesium is influenced by three factors: Peierls stress, dislocation source strength and GB resistance. Finally, El-Awady [33] extended the results of simulations dedicated to the effect of micropillar size effect and proposed a model based on dislocation density to predict the HP effect. In summary, much work has been done to reveal the dominant mechanisms responsible for the grain size effect, but no well-accepted conclusion has yet been achieved.

With the present work, we wish to bring new decisive elements clarifying key points of this long-standing problem. Our goal is not to carry out numerical simulations that are as accurate as possible, but rather to study simple config-

urations that allow us to decide between different scenarios. We have recently shown with 3D-DD simulation [34], that the HP law can be reproduced with simple polycrystalline aggregates made of cubic grains. In order to identify the underlying mechanisms controlling this simulated size effect, additional 3D-DD simulations were performed. In what follows, we explore the plastic properties of a cubic grain embedded in an elastic matrix. This simplification of the previous simulations still shows a grain size effect and strong similarities with the experimentally observed HP effect. Moreover, this configuration is theoretically equivalent to the problem of Eshelby’s inclusion that can be studied analytically. Owing to the simplicity of these configurations, one can use an original computational procedure recently proposed to compute the back stress induced by GNDs density evenly distributed over a surface [35]. From these, we want to probe the elementary mechanisms explaining the simulated HP effect. The rest of the paper is organized as follows. In Section 2, the simulation technique and conditions are presented. In Section 3, the simulation results are discussed. In Section 4, the conclusions we draw from this study are summarized.

2. Simulation conditions

In order to study the underlying mechanisms controlling the effect of grain size observed in [34], complementary 3D-DD simulations were performed. In the following, we explore the plastic properties of a cubic grain embedded in an elastic matrix. Such configuration is an extreme simplification of polycrystal mechanics, but it nevertheless presents a grain size effect which can be compared with the experimentally observed HP effect.

The open-source code *microMegas* was used to perform the 3D-DD simulations. The main features of this code are depicted in [36]. Pure copper is used as test case material with a lattice friction τ_0 fixed to 2.5 MPa. Six grain sizes between 1.25 μm and 10 μm are tested. We apply the same simulation protocol as the one used in [34]. A point to remember is that GBs are considered as impenetrable interfaces to the movement of the dislocations. This simplification

is physically justified since the simulated deformations are limited to 0.2% and therefore the applied stresses are relatively low and the plastic deformation is relatively homogeneous within the deformed grains.

In all the simulations, the dislocated grain under investigation is placed at the center of a large simulation volume with periodic boundary conditions. As the grain size is always two times smaller than the simulation volume and the elastic interactions between dislocations are cut at distances larger than the linear grain size, the mechanical problem under investigation is equivalent to a finite plastic volume embedded in infinite elastic medium. Hence, it is the equivalent of the Eshelby's inclusion problem, but solved at the dislocation scale with a discrete mechanical approach. No elastic strain incompatibility needs to be considered since linear elastic isotropy is used. Also, the plastic incompatibility between the deformed grain and the elastic medium is by definition accommodated by the geometrically necessary dislocations accumulated at grain boundaries.

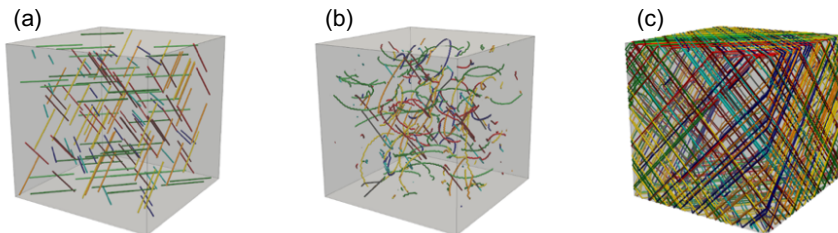


Figure 1: (a) Initial dislocation microstructure made of a random distribution of 168 FR sources. (b) the forest dislocation density (SSDs) in the interior of simulated grain at $\varepsilon_p = 0.2\%$. (c) the polarized dislocation density (GNDs) accumulated in the vicinity of GBs at $\varepsilon_p = 0.2\%$. Dislocations belonging to different slip systems are illustrated with different colors.

An example of the simulated initial dislocation microstructure is shown in Fig. 1a. This is a random distribution of screw FR sources belonging to the eight slip systems activated when tensile loading is applied in the [001] direction. The sources length L is set as a third of the grain size d . According to Ohashi *et al.* [27], this solution gives the lowest critical stress to activate plastic

deformation in a cubic grain. In line with [34], simulations are not made using a constant initial dislocation density with different grain sizes, but rather with a constant number of FR sources, i.e., 168 FR sources (21 per slip system). In this work, we are focused on exploring the size effects in small grains with relatively low dislocation density. The use of FR sources in the initial dislocation microstructure is then preferred as it allows introducing strong pinning points and avoids starvation effect. Hence, the initial dislocation density decreases with the grain size and is spanning from 10^{11} to $10^{13} m^{-2}$. This variation, imposed in the simulation setup is consistent with many experimental observations reported for micron-sized crystals [37–39] and fine-grained polycrystalline materials [40–42]. An increase of the dislocation density with decreasing grain sizes is indeed expected in volumes smaller than a few microns and can easily be justified with DD simulations. If a low initial dislocation density is taken into account in the simulations, regardless of grain size, then the smaller grains are free of dislocations and no plastic deformation (in the absence of specific dislocation nucleation processes) can be reproduced. On the other hand, if a high and constant initial dislocation density is used, a strong forest strengthening is then simulated and no more size effects are reproduced by modifying the grain size. The same remark has been made by El-Awady [33] for the modeling of plastic deformation in micron-sized crystals.

In Tab. 1, information regarding the grain size, the source length, the corresponding initial dislocation density and the strain rates used in this work is summarized.

The activation of cross-slip (CS) for screw dislocation lines is accounted for in the simulations following simulation rules described in [36]. According to many DD investigations (see for instance [43, 44]) CS is a key mechanism to simulate plasticity in micron-sized grains because it avoids the starvation of dislocation multiplication by creating new sources and strong pinning points in the dislocation microstructure.

d (μm)	L (μm)	ρ_{ini} (m^{-2})	$\dot{\epsilon}$ (s^{-1})
1.25	0.375	3.2×10^{13}	70
2.5	0.75	8×10^{12}	60
3.5	1.05	4×10^{12}	55
5	1.5	2×10^{12}	50
7.5	2.25	0.9×10^{12}	45
10	3	0.5×10^{12}	40

Table 1: Definition of the main quantities controlling the simulated microstructures. d is the grain size, L is the FR source length, ρ_{ini} is the initial dislocation density and $\dot{\epsilon}$ is the imposed plastic strain rate in the [001] grain orientation.

3. Results and discussion

A deformation, up to 0.2% of plastic strain, of the six different grains defined in Section 2 was simulated. As expected, these simulations show a grain size effect. As illustrated in Fig. 2, the flow stress at any fixed value of plastic strain increases as grain size is reduced. Moreover, the simulated flow stress is comparable to that of many experiments and is even stronger than that calculated in our previous study with periodic polycrystal aggregates [34].

From the simulated stress-strain curves shown in Fig. 3a, another important feature should be noted. The stress-strain curves obtained with different grain sizes are parallel and the strain hardening rate is independent of the dislocation density. A constant strain hardening rate is then systematically observed at low plastic strain. Such behavior is in agreement with some experimental stress-strain curves observed in the early stage of deformation found in 316L steels [8] or bainitic steels [42]. Furthermore, we see in Fig. 3a that the simulated size effect is directly related to a change of the yield stress at the very beginning of the stress-strain curves. In order to unravel these observations, a systematic analysis of the different mechanisms controlling plastic strengthening is made in the following.

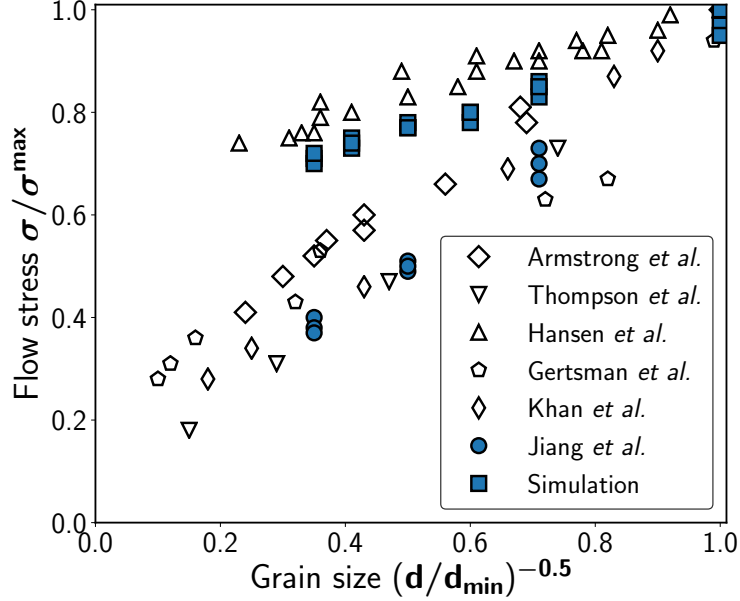


Figure 2: Scaled data demonstrating the Hall–Petch effect in experiments (open marks), in the 3D-DDD simulations reported in [34] (filled circles) and in the present study (filled squares). Each data set is scaled by its minimum grain size and maximum flow stress (measured at 0.2% plastic strain) in order to compare all data sets on the same axis.

3.1. Origin of the constant strain hardening rate

Inside the plastically-deformed grain, two families of dislocations with different properties can be considered: the statistically stored dislocations (SSD) and the geometrically necessary dislocations (GND). The way we define the areas where SSDs and GNDs are stored during plastic deformation is explained with details in [35]. As an example, Fig. 1 shows that the SSD density ρ_{SSD} (alternatively called forest dislocation density) is inside the grain and the GND density ρ_{GND} (alternatively called polarized dislocation density) accumulates near the GBs. Those two dislocation densities contribute to plastic strengthening in different ways.

The internal stress τ_{int} opposed to plastic flow inside the grains results from two contributions. One is a short-range stress τ_{SSD} associated with dislocations contact reactions and this stress is a function of only ρ_{SSD} since polarized

dislocations can hardly form junctions. The other is a long-range stress τ_{GND} associated with the density ρ_{GND} accumulated at GBs. Since the evolution of the SSD and GND density can be directly calculated, an average value of τ_{int} is defined in the simulations assuming that the contributions of τ_{SSD} and τ_{GND} are additive. This hypothesis has been validated for this study on the condition that the strain rate imposed during the simulations is low enough to reproduce quasi-static dislocation dynamics. In this case, $(\tau_{SSD} + \tau_{GND})$ calculated at the grain center almost perfectly balances the applied stress τ_{app} imposed during grain deformation.

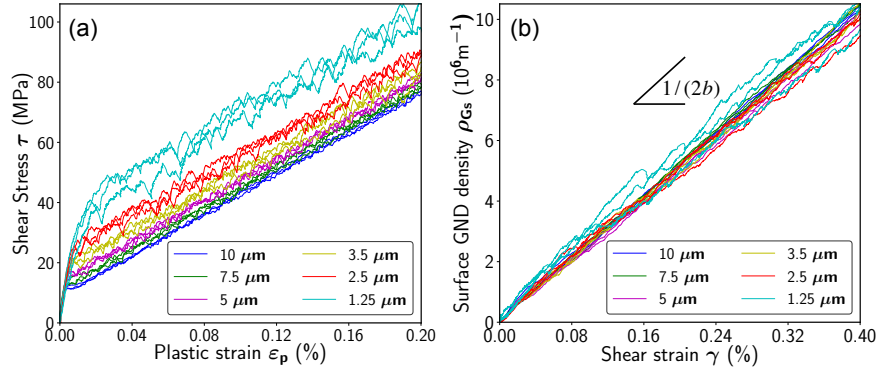


Figure 3: Simulations results for cubic grains with different sizes and deformed in the [100] tensile direction. (a) Evolution of the applied shear stress resolved on the active slip systems, τ_{app} as a function of the plastic strain ϵ_p in the [100] direction. (b) Concomitant variations of the surface dislocation density ρ_{Gs} as function of the resolved plastic shear strain γ .

In all the simulations, we found that ρ_{SSD} hardly evolves inside the grains. Up to 0.2%, ρ_{SSD} is constant and stay very close to the initial dislocation density ρ_{ini} . This observation is consistent with the initial dislocation density used in our simulations, i.e. a constant small number of sources is considered within the grains. τ_{SSD} is then almost constant and its amplitude corresponds to the yield strength measured on the stress-strain curves before accumulating GND density. This lack of forest strengthening implies that the evolution of τ_{GND} is dominant in controlling strain hardening in the simulations. Surprisingly, as shown in Fig. 3a, τ_{GND} is independent of grain size and its variation is linearly

proportional to ε_p .

More detailed analysis of the simulations shown that the long-range stress τ_{GND} associated with the GND density is a load-sensitive stress. In the simulated grains, τ_{GND} is systematically opposed to the applied resolved shear stress. This is why, τ_{GND} is sometimes referred to as “back stress” in the following.

We now recall the main steps in calculating τ_{GND} in the DD simulations. In our previous work [35], the distribution of GNDs from GB surface to the inner area of a grain is evaluated and the GNDs density is found concentrated at a thin GBs area of $0.4 \mu m$ thick, which is about $1/25$ of the simulated grain size $10 \mu m$. This proportionality between the thickness of GBs area and the grain size is applied in this work. The spatial distribution of GNDs density $\underline{\alpha}$ is computed in the wall-like GB area using the formulation established by Arsenlis and Parks [45]. Then, $\underline{\alpha}$ is multiplied with the GB area thickness and that determines a local GND density variation at lower scale. By doing such calculations, a surface Nye’s tensor $\underline{\alpha}_s$ is defined as:

$$\underline{\alpha}_s = \sum_i^n \rho_{G_s}^i (\underline{\mathbf{b}}^i \otimes \underline{\mathbf{l}}^i) \quad (2)$$

where $\rho_{G_s}^i$ is the surface GND density calculated as the total length of GND segments accumulated against the GBs and divided by the surface area of each GB facets enclosing a grain. $\underline{\mathbf{b}}^i$ and $\underline{\mathbf{l}}^i$ are the normalized Burgers vector and line direction vector for slip system i , respectively. Once $\underline{\alpha}_s$ is known, the elastic distortion tensor $\underline{\mathbf{U}}_e$ is calculated by integrating equation $\underline{\alpha}_s \simeq \text{curl} \underline{\mathbf{U}}_e$. This calculation is made assuming a Dirac delta distribution of the GND density at the GBs. This solution is a common approximation which allows for the identification of analytical solutions in the case of infinite dislocation walls [46, 47]. Then, assuming isotropic elasticity, the back stress associated with each GB facets can be calculated inside the grain using the stress solution for the infinite dislocation walls and dimensionless shape functions recently developed to calculate the self-stress of interfacial finite dislocation walls with any character [35]. Here, it is important to note that none of the steps in the calculation summarized above involve grain size. Thus, the back stress at the center of a

grain is only proportional to the surface GNDs density ρ_{Gs} stored at the GBs. For this reason, identifying the evolution of back stress with plastic deformation or strain-hardening requires only a calculation of the evolution of the surface GND density the GBs.

To proceed with such a calculation, it should be noted that the density of surface GND ρ_{Gs} is of dimension m^{-1} and differs from the conventional dislocation density ρ with dimension m^{-2} . Monitoring ρ_{Gs} as a function of γ in the DD simulations can simply be implement (see [35]). The result of such calculation with the six simulated grain sizes is shown in Fig. 3b. As the forest hardening inside the grains is extremely low, a simple model is proposed to understand the reported behavior. Inside a cubic grain of size d with fcc lattice symmetry, when a dislocation loop at grain center expands to the GBs, the increase of ρ_{Gs} is approximately $d\rho_{Gs} = 1/(\sqrt{2}d)$ and the shear strain made by the expansion of this loop is $d\gamma = (3\sqrt{3}b)/(4d)$. The storage rate of surface GND density is therefore whatever the number of active slip systems and the grain size:

$$\frac{d\rho_{Gs}}{d\gamma} = \frac{2\sqrt{6}}{9b} \approx \frac{1}{2b} \quad (3)$$

The relationship established in Eq. 3 is an essential property of ρ_{Gs} . Contrary to the classical storage rate of the dislocation density in a volume, which is inversely proportional to the grain size d , the storage rate of the surface GND density $d\rho_{Gs}/d\gamma$ is independent of the grain size and it is a constant quantity of the order of $(2b)^{-1}$. This property simply explain why we observe in the simulations that all simulated grains (shown in Fig. 3b) collapse into a single trend line. The storage rate of the surface GND density is, during the plastic deformation of the grains, a constant quantity which is independent of the grain size. It should be noted that the DD simulation results reproduced here are in quantitative agreement with the simple dimension analysis leading to Eq. 3.

The back stress inside a deformed grain being proportional to ρ_{Gs} , the work hardening generated by the accumulation of GND density is also a constant and is expected to be independent of the grain size. This explains why in the absence

of forest hardening a constant linear relationship is observed between τ and ε_p (Fig. 3a). This result is general and was verified at low strain in different DD simulations considering periodic aggregates made of several cubic grains [34]. This important result provides a physically justified argument to understand the independence of the HP constant K with plastic strain reported in some experiments (see for instance [17]).

3.2. Influence of the initial dislocation microstructure

In the previous section, we established that the strain hardening reproduced in the DD simulations do not explain the observed size effect (Fig. 2). We now investigate the possibility that this effect is connected to the dislocation properties controlling the flow stress amplitude at plastic yield.

In the theoretical work of Zaiser and Sandfeld [48], a similitude principle is applied to show that grain size effect should scale with $D\sqrt{\rho}$. Such prediction was confirmed by different works. For instance, El-Awady [33] deduced the same scaling law from DD simulation made with micro crystals with different size. Haouala *et al.* [49] also reported the same type of behavior from strain gradient CP-FFT simulations. Here it must be noted that in such works, the initial dislocation density was considered constant imposing a systematic variation of $D\sqrt{\rho}$. In the present study, the number of initial sources n and the proportionality between the source length and the grain size are set constant. With such initial simulation conditions, $D\sqrt{\rho}$ is constant and equals $\sqrt{n/3}$. Nevertheless a size effect is produced (see Fig. 3). This suggests that the size effect we simulated may not be simply controlled by the dislocation density normalized by the grain size. Some other mechanisms may be involved in the plastic strengthening to give rise to a size effect. For this reason, the influence of the initial dislocations microstructure is analyzed with some details in the following.

The dislocation microstructure used at the beginning of the simulations is presented in Section 2 and summarized in Tab 1. Only two basic properties may control the flow stress with such microstructures. Either the plastic yield instability is reached when the applied stress equals the critical stress needed

to activate FR sources [50], or when it equals the critical stress needed to unzip the dislocation junctions formed at the very beginning of the simulations to minimize the elastic energy [51]. The predominance of one or the other of these mechanisms results from the choice of the length of FR sources in relation to the mean distance between dislocation lines. The latter quantity is statistically fixed by the initial dislocation density [52].

In the source control regime, a minimum stress is required to bow out the dislocation sources to a critical position where the irreversible expansion of dislocation loops is triggered [53]. Such critical stress can be predicted with the Foreman equation [50]:

$$\tau_F = A \frac{\mu b}{2\pi L} \left[\ln \left(\frac{L}{r_0} \right) + B \right] \quad (4)$$

for screw dislocations $A = 1.5$; for edge dislocations $A = 1$. In the case of FR sources with finite pinning points, B is commonly considered as 0 and the core radius of dislocation r_0 is considered as b . The characteristic length of the FR sources imposed in the initial configuration is denoted by L .

In the forest control regime, the stress to unzip dislocation junctions anchoring dislocation lines in their glide plane depends on the dislocation density and can be predicted with the forest equation [51, 54, 55]:

$$\tau_{forest} = \alpha \mu b \sqrt{\rho} \quad \text{with} \quad \alpha = \frac{\ln(\alpha_{ref} b \sqrt{\rho})}{\ln(\alpha_{ref} b \sqrt{\rho_{ref}})} \alpha_{ref} \quad (5)$$

In Eq. 5, the reference forest strength coefficient approximates to $\alpha_{ref} = 0.35$ at the reference dislocation density $\rho_{ref} = 10^{12} m^{-2}$.

In the present study, a proportionality rule between the grain size d and the length of the FR sources L is assumed in the initial configuration and $L = d/3$. Also, the number of sources n in the initial configuration is identical in all the simulations. Thus, the initial dislocation density ρ_{ini} is expressed as:

$$\rho_{ini} = \frac{nL}{d^3} = \frac{n}{27L^2} \quad (6)$$

In Fig. 4, the critical resolved shear stress (CRSS) averaged with 3 different initial configurations for the different grain sizes is reported. The simulation

results are compared with the predictions of the Foreman equation (Eq. 4) and the forest equation (Eq. 5). As expected, the dislocation density in the grains being initially small, the calculated yield stress are in better agreement with the prediction of the Foreman equation. This indicates that the property controlling the initiation of plastic deformation in the simulated grains is preferentially source multiplication. However, it must be noted that the simulated CRSS shift towards the prediction of the forest equation when the grain size is decreasing, i.e., when ρ_{ini} is increasing. Additionally, to test the additivity of the source strengthening and forest strengthening effects, a quadratic mean of the Foreman equation and the forest equation is calculated using $\sqrt{(\tau_F^2 + \tau_{forest}^2)}/2$. The corresponding predictions are plotted with black dashed line in Fig. 4. It can be seen that the prediction of the quadratic mean is in very good agreement with the DD simulations results when the grain sizes are small. Hence, the source and forest strengthening mechanisms are both contributing to the flow stress and their respective contribution can be captured with a simple rule of mixture. However, the prediction of the quadratic mean becomes poorer and poorer as the grain size increases. This result implies that the CRSS of the larger simulated grains is mainly controlled by the length of the dislocation sources in the initial microstructure and that the mechanisms of plastic relaxation existing at the very beginning of plastic strain poorly affect the flow stress.

From the above analysis, one can conclude that in fine grains (in the micrometer range) and with a low initial dislocation density, CRSS is dominated by the multiplication of dislocation sources. It is questionable whether this result is dependent on the method used to construct the initial dislocation microstructure. Here, we insist on the fact that the dislocation microstructure used at the beginning of the simulations must be considered as the minimum dislocation density necessary to allow the grains to deform in multiple slip. This last condition is important to mechanically accommodate the deformation incompatibilities existing at GBs during the deformation of polycrystalline aggregates.

To build an initial microstructure where plastic strain is dominated by the forest mechanism would impose a dislocation density multiplied by a factor

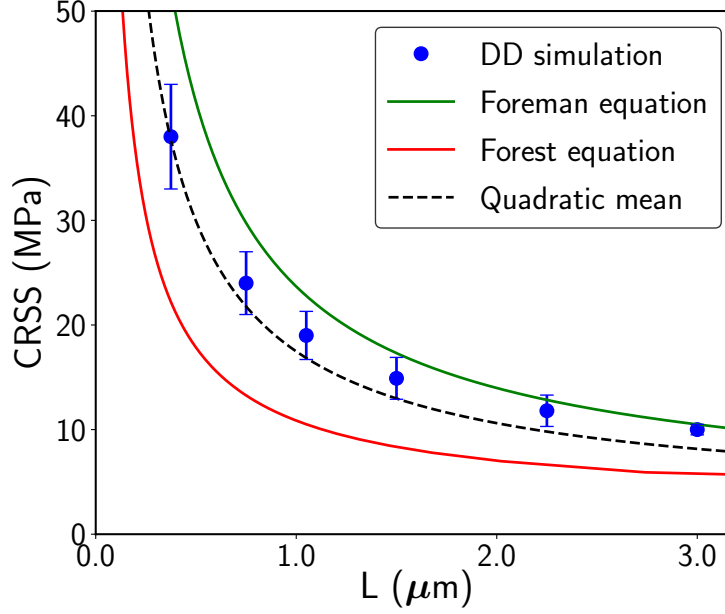


Figure 4: Variation of the mean CRSS as a function of FR source length L . The mean CRSS evaluated from the stress-strain curves in Fig. 1 are plotted with blue symbols and error bars are estimated from the highest and lowest CRSS simulated with a given FR source length. The theoretical predictions calculated from the Foreman equation (Eq. 4) and the forest equation (Eq. 5) are plotted with green and red lines, respectively. A dry friction τ_0 of 2.5 MPa is taken into account. In addition, a quadratic mean is evaluated from the Foreman equation and the forest equation with $\sqrt{(\tau_F^2 + \tau_{forest}^2)}/2$ and the obtained results are shown with black dashed line.

greater than 10. As shown in Tab 1, this solution seems unrealistic as the dislocation density in the smallest simulated grains is already very high. Moreover, the flow stress at plastic yield is always low enough to rule out the possibility of dislocations nucleation at GBs. Therefore, we propose that the prediction of plasticity dominated by the multiplication of dislocations from a few sources is realistic at the early stages of plastic deformation and for grain sizes in the micrometer range.

We have therefore identified a simple mechanism that justify the existence of a grain size effect. This result is in agreement with El-Awady's recent results in the case of micropillar plasticity, which he used to justify the existence of the

classical HP law in polycrystals [33]. In order to take this analysis a step further, it should be noted here that the initial dislocation microstructure existing in the grains seems to be a key material parameter for understanding the detail nature of the HP law. In the next section, we show that the results of our DD simulations can explain some experimentally observed deviations from the HP law.

3.3. Identification of the size effect scaling law

So far, we shown that (i) the strain hardening mechanism associated with the accumulation of GNDs against GBs is constant at low stress and cannot explain the existence of a grain size effect, (ii) the existence of the HP law must rather be explained by the differences in flow stress amplitudes at yield. Among the sources multiplication and the forest mechanism, DD simulations suggest that the former mechanism is the most plausible with grains in the micrometer range. Therefore, the scaling law associated with the grain size effect should theoretically be consistent with an equation of the form¹:

$$\tau \propto \ln\left(\frac{L}{b}\right) \frac{1}{L} \propto \ln\left(\frac{d}{b}\right) \frac{1}{d} \quad (7)$$

This prediction is in good agreement with the recent work of Li *et al.* [17], who gathered a wide range of experimental data and tested several grain size dependent relationships, such as $1/\sqrt{d}$, $1/d$ and $\ln(d/b)(1/d)$. The one in form $\ln(d/b)/d$ provides the best fit with the experimental data. Now, we test the same systematic approach with the DD simulation results.

In Fig. 5, the flow stress values taken from Fig. 3 at 0.1% and 0.2% of plastic strain are plotted. Two functions of the form: $a + b/\sqrt{d}$ and $a + b[\ln(d/b)/d]$ are first used to adjust the two set of 18 simulations results. The fit calculation we have performed only imposes that the two sets of curves agree with the results of the DD simulations for the largest grain size, i.e. the one where the

¹It is interesting to note that a plastic flow controlled by the forest mechanism provides the same equation form since $\alpha \propto \ln(d/b)$ and $\rho_{ini} \propto 1/d^2$ in Eq. 5-6.

ε_p	$R^2(1/\sqrt{d})$	$R^2(1/[\ln(d/b)/d])$	$R^2(1/d^n)$
0.1%	0.97	0.95	0.99
0.2%	0.95	0.94	0.99

Table 2: The calculated coefficients of determination R^2 for the fitting results with form $1/\sqrt{d}$, $1/[\ln(d/b)/d]$ and $1/d^n$ shown in Fig. 5 are summarized.

dispersion of the simulation results is minimal. As reported in Tab. 2 giving the coefficient of determination R^2 calculated for each fitting, the difference between the two tested scaling law is small. Nevertheless, for both tested plastic strain amplitudes (0.1% and 0.2%), the $1/\sqrt{d}$ form is found to give a slightly better correlation with the simulation results.

Hence, the size effect reproduced in the DD simulations appears to be in better agreement with the conventional formulation of the HP law rather than the solution, Eq. 7 one can expect from a theoretical analysis.

In order to give an ultimate fit to the simulation data, a third function of form $\tau_0 + k/d^n$ is tested and the fitting results are reported in Fig. 5 with orange dash-dotted lines. As noted in Tab. 2, this last fit gives an coefficient of determination $R^2 = 0.99$. We obtained an exponent $n = 0.64$ at 0.1% of plastic strain and an exponent $n = 0.67$ at 0.2% of plastic strain. Hence, both values are closed to the exponent of 0.5 considered in the conventional HP law. From a practical point of view, the difference between this scaling law we fitted on the simulation data and the HP law could hardly be differentiated by experimental means.

To understand the origin of this deviation from the theoretical law expected in the DD simulations, we now analyze the evolution of the dislocation microstructure inside grains with two different sizes, i.e. $d = 1.25 \mu m$ and $d = 10 \mu m$. To precisely characterize the distribution of source lengths inside the grains at yield, we calculated at the time step when a first dislocation loop is deposited at the GB, the length of all the curved dislocation lines within the microstructure. Such segments are ended either by junctions, or by points

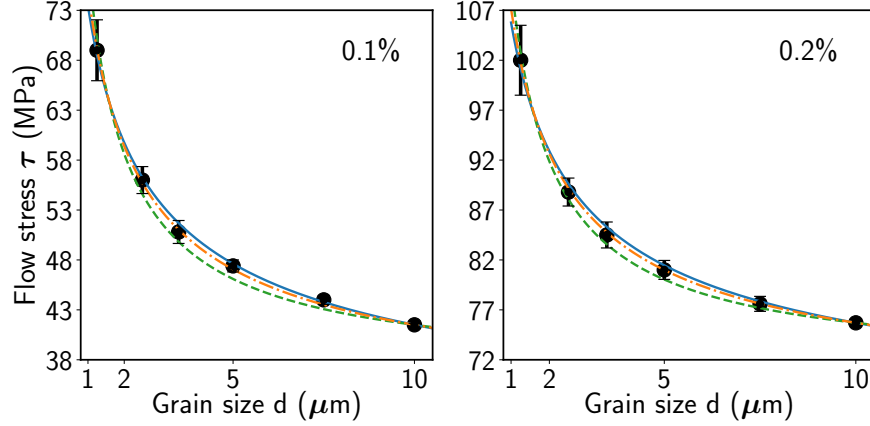


Figure 5: Variation of the simulated flow stress as function of the grain size, measured at 0.1% and 0.2% of plastic strain. First, the simulation results (squares) are fitted with 2 mathematical forms: $a + b/\sqrt{d}$ (blue full line) and $a + b \ln(d/b)/d$ (green dashed line), a and b are fitting parameters. Then, a third ultimate fit (orange dash-dotted line) is performed with form $\tau_0 + k/d^n$, where τ_0 is the mean value of a from the above two fitting results and k and n are fitting parameters.

at the intersection between two glide planes or by the initial pinning points introduced in the initial random configuration made with the n FR sources.

The corresponding histograms are plotted in Fig. 6. As we can see, the length distribution inside the small grain is much more spread out, while the length distribution in the large grain is concentrated inside a narrow range. More precisely, in the large grain, the length distribution is located in a range between 3 and 4 μm , close to the length of FR sources introduced in the initial configuration (see Tab. 1). On the other hand, in the small grain, the set of columns located out of 0.5 μm is not negligible. It indicates that a few sources, with a length longer than the initial value (0.375 μm), are formed during the very first steps of the dislocation dynamics. The flow stress in such grain is then smaller than expected since dislocation multiplication can occur from longer dislocation segments. This result justifies the systematic deviation observed in Fig. 4 for the smaller grains with respect to the prediction of the Foreman's equation (Eq. 4). Indeed, the formation of long sources (relative to

grain size) is more likely to be observed in the smaller grains since in these grains the dislocation density is higher, the dislocation line tension is less rigid, the internal stress is higher and the cross-slip of the screw dislocations is facilitated.

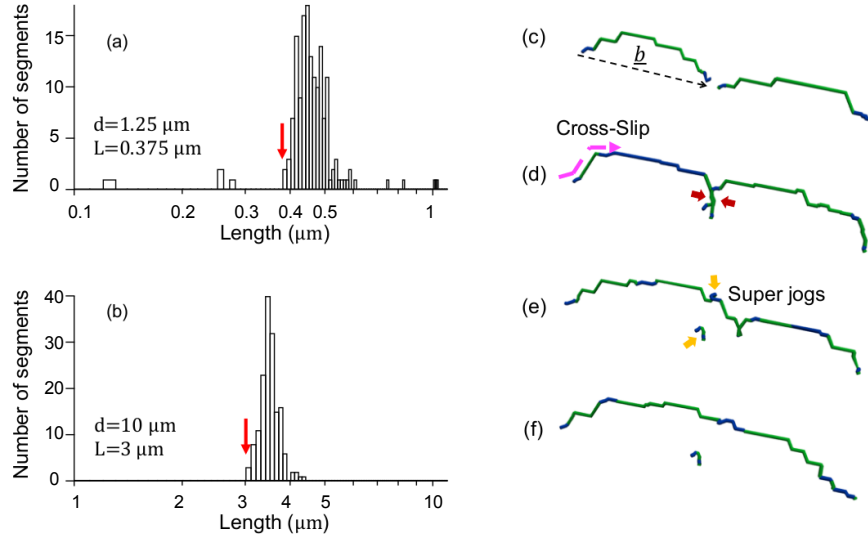


Figure 6: Length distribution of pinned dislocation line segments in (a) a small grain $d = 1.25 \mu\text{m}$ and (b) a large grain $d = 10 \mu\text{m}$. Those distribution are calculated when a first dislocation loop is deposited at the GBs. The formation of a long segment observed in the smaller grain at the beginning of the simulation is illustrated with snapshot images displayed in (c)-(f). The screw direction (parallel to \underline{b}) is indicated in (c). Segments in different glide planes are noted with different colors. In (d), a double cross-slip is illustrated and strong attractive forces between close segments of opposite sign are marked with red arrows. The contact reaction observed in (d) is a collinear annihilation. In (e), a longer line segment is formed after the reaction. The two super-jogs involved in the collinear annihilation are noted with yellow arrows. In (f), the formed long segment expands rapidly.

To depict the process of long source formation, we provide some evidence of the rearrangement of the dislocation microstructure in the small grain $d = 1.25 \mu\text{m}$. This process is illustrated in Fig. 6(c-f) with a snapshot made of four images. In this sequence, two pinned segments close to the screw direction interact and annihilate with a collinear reaction [56]. The process goes as follows. In Fig. 6d, owing to a double cross-slip process, two super jogs are formed along

one dislocation line. The presence of those super jogs allows two attractive line segments to interact and annihilate with a collinear reaction. In Fig. 6e, we see that this annihilation reaction leaves a tiny line segment and a long dislocation segment pinned at its ends. At last in Fig. 6f, this long segment bows-out and acts as a source. It expands rapidly because the multiplication of this dislocation segment is made possible at a lower stress.

Such rearrangement processes are frequently observed in the simulations of smaller grains. This explains why the scaling law for the grain size effect does not agree with a $[\ln(d/b)/d]$ form. Rather, this scaling law agrees with a $1/\sqrt{d}$ form, which takes into account the enhanced relaxation of dislocation microstructures when decreasing the grain size. Such effect can be characterized inside the smaller grains by an increase in the ratio between the active dislocation source length and the grain size dimension. Lastly, it is important to note that the simulations performed with a constant initial dislocation density with increasing grain sizes will not lead to the same conclusion.

4. Conclusions

A large set of DD simulations dedicated to the configuration of a plastically-deformed cubic grain within an elastic matrix were performed to study the physical origins of the HP effect. At low strain, the evolution of surface GNDs density is much higher than the one of SSDs density; therefore the strengthening and the strain hardening are mainly controlled by the back stress generated by GNDs rapidly accumulated at GBs. We show that the storage rate of surface GND density is constant and independent of grain size. Such result is verified by both simple geometrical analysis and DD simulations. As a consequence, the computed strain hardening rate shows no sensitivity to grain size in all the simulated grains when deformed in multislip conditions. Such finding suggests that numerically the back stress due to the plastic incompatibility developed at GBs could be evaluated directly from the evolution of the total plastic strain inside grains.

The size effect reproduced with DD simulations is related to the calculated CRSS at the very beginning of plastic deformation. A refined investigation was made to quantify the influence of the initial dislocation microstructure on the CRSS. Particularly, two strengthening mechanisms existing at the initiation of plastic deformation are studied: the dislocation source strengthening and the dislocation forest strengthening. Both mechanisms suggest that the variation of the CRSS with grain size should be governed by the form $\ln(d/b)(1/d)$. However, the HP relationship calculated with DD simulations is in better agreement with the form $1/\sqrt{d}$. Such discrepancy is explained by a rearrangement of the initial dislocation microstructure at the beginning of the simulations mainly to relax the elastic energy inside the grain. The rearrangements are more active in the small grains and driven by line tension, collinear annihilation and cross-slip effects. It should be noted that the determination of scaling law might be influenced by some simulation simplifications, e.g. grains are in cubic shape, impenetrable GBs are considered and long-range internal stress is only associated with the GNDs density accumulated at GBs. These simplifications are justified for the micron-sized grains at low plastic strain explored in this work. However, in order to investigate the general HP law at a larger range of grain sizes, the impact of the used simulation simplifications should be carefully addressed in future work.

The range of grain sizes explored in this work is limited to several micrometers and the dislocation density used in simulations varies with grain size. When extending our discussions to the case of coarse-grained polycrystals, the arguments we made from the DD simulations may be found incomplete. In industrial alloys, the initial dislocation density is expected of the same order of magnitude and the confined effect of source length is negligible. In this case, no size effect is predicted from the present simulation analysis, which is however in contradiction with many experimental facts. Therefore, the important issues concerning the localization of the plastic deformation in large grains and the associated formation of dislocation pile-ups at GBs should be a key issue with industrial polycrystalline materials. Those phenomena can lead to a heterogeneous dis-

tribution of GNDs density at GBs that possibly enables the transmission of dislocations. To justify the HP effect for larger grain sizes with a realistic initial dislocation density, we believe that the classical model of dislocation pile-up could be used as a criterion for defining the minimum stress for plastic slip transfer to the GBs. This solution would be necessary above a critical dimension when any change in grain size does not mechanically impose a change in the initial dislocation density.

In this work, we have shown that the physical properties behind the effect of grain size is complex despite the simple form of the HP law. Several dislocation mechanisms may be involved at the same time and the dominant one must be differentiated according to the explored grain size range and material history. This work also highlights the possibility of developing, based on the results of DD simulations, a simple dislocation density based model taking into account the elementary mechanisms controlling the grain size effect in polycrystalline materials. The strengthening effects we discussed are limited to dislocations confined within one grain. To further investigate the generalized size effect of polycrystalline aggregates, the sensitivity of plastic strengthening to crystallographic orientations also needs to be considered. Such effect is investigated in a forthcoming paper, which presents a new dislocation density-based model, justified by the results of the present study and making use of the surface GND density model we developed in [35].

References

- [1] E. Hall, The Deformation and Ageing of Mild Steel: III Discussion of Results, Proc. Phys. Soc., Sect. B 64 (1951) 747.
- [2] N. Petch, The Cleavage Strength of Polycrystals, J. Iron Steel Inst. 174 (1953) 25.
- [3] R. Armstrong, I. Codd, R. M. Douthwaite, N. J. Petch, The plastic deformation of polycrystalline aggregates, Philos. Mag. 7 (1962) 45.

- [4] A. Lasalmonie, J. Strudel, Influence of grain size on the mechanical behaviour of some high strength materials, *J. Mater. Sci.* 21 (1986) 1837–1852.
- [5] N. Hansen, Hall-petch relation and boundary strengthening, *Scr. Mater.* 51 (2004) 801–806.
- [6] R. Armstrong, Engineering science aspects of the Hall–Petch relation, *Acta Mech.* 225 (2014) 1013–1028.
- [7] Z. Cordero, B. Knight, C. Schuh, Six decades of the Hall–Petch effect – a survey of grain-size strengthening studies on pure metals, *Int. Mater. Rev.* 61 (2016) 495–512.
- [8] X. Feaugas, H. Haddou, Grain-size effects on tensile behavior of nickel and AISI 316L stainless steel, *Metall. Mater. Trans. A* 34 (2003) 2329–2340.
- [9] N. Tsuchida, H. Masuda, Y. Harada, K. Fukaura, Y. Tomota, K. Nagai, Effect of ferrite grain size on tensile deformation behavior of a ferrite-cementite low carbon steel, *Mater. Sci. Eng. A* 488 (2008) 446–452.
- [10] W. Baldwin, Yield strength of metals as a function of grain size, *Acta Metall.* 6 (1958) 139–141.
- [11] H. Conrad, Effect of grain size on the lower yield and flow stress of iron and steel, *Acta Met.* 11 (1963) 75–77.
- [12] U. Kocks, The relation between polycrystal deformation and single-crystal deformation, *Met. Mater. Trans.* 1 (1970) 1121.
- [13] T. Christman, Grain boundary strengthening exponent in conventional and ultrafine microstructures, *Scr. Metall. Mater.* 28 (1993) 1495–1500.
- [14] M. Ashby, The deformation of plastically non-homogeneous materials, *The Philosophical Magazine: A Journal of Theoretical Experimental and Applied Physics* 21 (1970) 399–424.

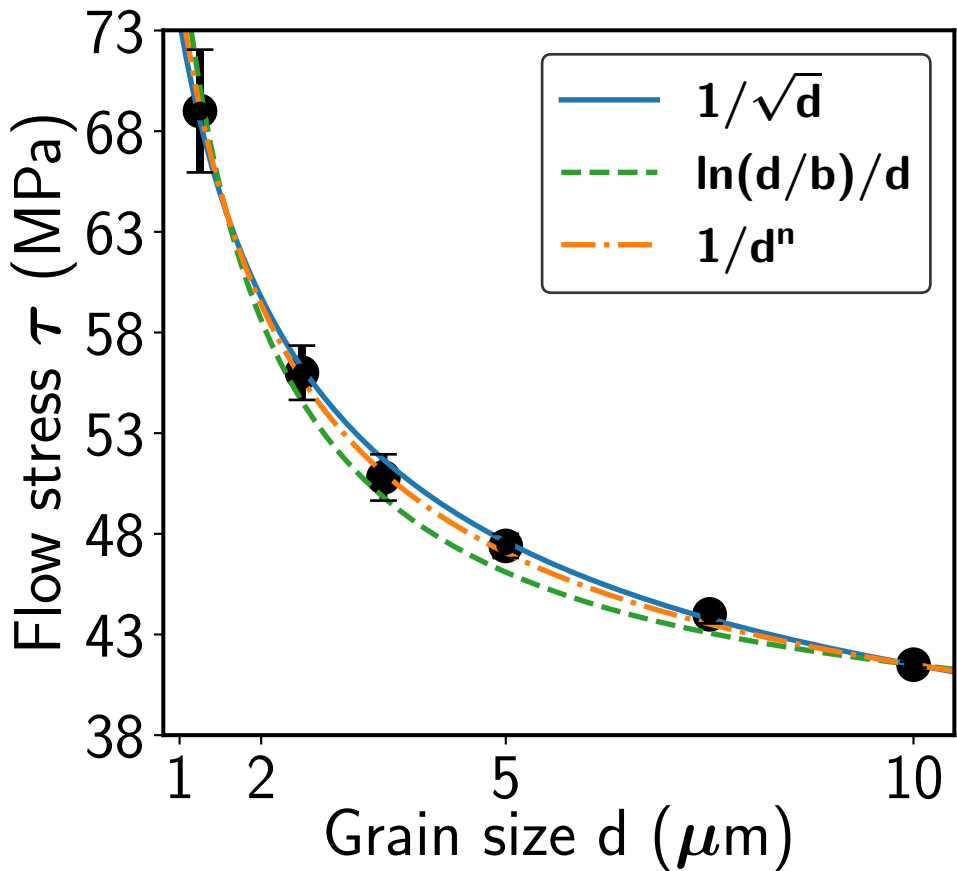
- [15] D. Dunstan, A. Bushby, Grain size dependence of the strength of metals: The Hall-Petch effect does not scale as the inverse square root of grain size, *Int. J. Plast.* 53 (2014) 56–65.
- [16] Y. Li, A. Bushby, D. Dunstan, The hall-petch effect as a manifestation of the general size effect, *Proceedings of the Royal Society A: Mathematical, Physical and Engineering Sciences* 472 (2016) 20150890.
- [17] Y. Li, A. Bushby, D. Dunstan, Factors determining the magnitude of grain-size strengthening in polycrystalline metals, *Materialia* 4 (2018) 182 – 191.
- [18] H. Van Swygenhoven, Grain boundaries and dislocations, *Science* 296 (2002) 66.
- [19] M. Dewald, W. Curtin, Multiscale modelling of dislocation/grain-boundary interactions: I. Edge dislocations impinging on $\Sigma 11$ (1 1 3) tilt boundary in Al, *Model. Simul. Mater. Sci. Eng.* 15 (2007) S193.
- [20] J. Wang, I. Beyerlein, C. Tomé, Reactions of lattice dislocations with grain boundaries in Mg: Implications on the micro scale from atomic-scale calculations, *Int. J. Plast.* 56 (2014) 156–172.
- [21] Z. Zhang, C. Shao, S. Wang, X. Luo, K. Zheng, H. Urbassek, Interaction of dislocations and interfaces in crystalline heterostructures: A review of atomistic studies, *Crystals* 9 (2019) 584.
- [22] S. Biner, J. Morris, A two-dimensional discrete dislocation simulation of the effect of grain size on strengthening behaviour, *Model. Simul. Mater. Sci. Eng.* 10 (2002) 617.
- [23] L. Nicola, E. Van der Giessen, A. Needleman, Size effects in polycrystalline thin films analyzed by discrete dislocation plasticity, *Thin Solid Films* 479 (2005) 329 – 338.
- [24] S. Lefebvre, B. Devincere, T. Hoc, Yield stress strengthening in ultrafine-grained metals : A two-dimensional simulation of dislocation dynamics, *J. Mech. Phys. Solids* 55 (2007) 788–802.

- [25] D. Balint, V. Deshpande, A. Needleman, E. V. der Giessen, Discrete dislocation plasticity analysis of the grain size dependence of the flow strength of polycrystals, *International Journal of Plasticity* 24 (2008) 2149 – 2172.
- [26] Z. Li, C. Hou, M. Huang, C. Ouyang, Strengthening mechanism in micro-polycrystals with penetrable grain boundaries by discrete dislocation dynamics simulation and hall–petch effect, *Computational Materials Science* 46 (2009) 1124 – 1134.
- [27] T. Ohashi, M. Kawamukai, H. Zbib, A multiscale approach for modeling scale-dependent yield stress in polycrystalline metals, *Int. J. Plast.* 23 (5) (2007) 897–914.
- [28] C. de Sansal, B. Devincere, L. Kubin, Grain size strengthening in micro-crystalline copper: A three-dimensional dislocation dynamics simulation 423 (2010) 25–32.
- [29] C. Zhou, R. Lesar, Dislocation dynamics simulations of plasticity in polycrystalline thin films, *Int. J. Plast.* 30-31 (2012) 185–201.
- [30] R. Yellakara, Z. Wang, A three-dimensional dislocation dynamics study of the effects of grain size and shape on strengthening behavior of fcc Cu, *Comput. Mater. Sci.* 87 (2014) 253–259.
- [31] X. Zhang, K. Aifantis, J. Senger, D. Weygand, M. Zaiser, Internal length scale and grain boundary yield strength in gradient models of polycrystal plasticity: How do they relate to the dislocation microstructure?, *J. Mater. Res.* 29 (2014) 2116–2128.
- [32] H. Fan, S. Aubry, A. Arsenlis, J. El-Awady, Orientation influence on grain size effects in ultrafine-grained magnesium, *Scr. Mater.* 97 (2015) 25–28.
- [33] J. El-Awady, Unravelling the physics of size-dependent dislocation-mediated plasticity, *Nat. Commun.* 6 (2015) 5926.

- [34] M. Jiang, B. Devincere, G. Monnet, Effects of the grain size and shape on the flow stress: A dislocation dynamics study, *Int. J. Plast.* 113 (2019) 111–124.
- [35] M. Jiang, G. Monnet, B. Devincere, Stress fields of finite-size dislocation walls and prediction of back stress induced by geometrically necessary dislocations at grain boundaries, *Journal of the Mechanics and Physics of Solids* 143 (2020) 104071.
- [36] B. Devincere, R. Madec, G. Monnet, S. Queyreau, R. Gatti, L. Kubin, *Mechanics of Nano-objects*, Presses de l’Ecole des Mines de Paris, 2011, Ch. Modeling crystal plasticity with dislocation dynamics simulations: The ‘microMegas’ code.
- [37] P. Ambrosi, W. Homeier, C. Schwink, Measurement of dislocation density in [100]- and [111]- copper single crystals with high relative accuracy, *Scr. Metall.* 14 (1980) 325–329.
- [38] R. Gu, A. Ngan, Effects of pre-straining and coating on plastic deformation of aluminum micropillars, *Acta Mater.* 60 (2012) 6102–6111.
- [39] J. El-Awady, M. Uchic, P. Shade, S. Kim, S. Rao, D. Dimiduk, C. Woodward, Pre-straining effects on the power-law scaling of size-dependent strengthening in Ni single crystals, *Scr. Mater.* 68 (2013) 207–210.
- [40] N. Kamikawa, X. Huang, N. Tsuji, N. Hansen, Strengthening mechanisms in nanostructured high-purity aluminium deformed to high strain and annealed, *Acta Materialia* 57 (2009) 4198–4208.
- [41] H. Adachi, Y. Miyajima, M. Sato, N. Tsuji, Evaluation of dislocation density for 1100 aluminum with different grain size during tensile deformation by using in-situ x-ray diffraction technique, *Mater. Trans.* 56 (2015) 671–678.
- [42] S. He, B. He, K. Zhu, M. Huang, Evolution of dislocation density in bainitic steel : Modeling and experiments, *Acta Mater.* 149 (2018) 46–56.

- [43] A. Hussein, S. Rao, M. Uchic, D. Dimiduk, J. El-Awady, Microstructurally based cross-slip mechanisms and their effects on dislocation microstructure evolution in fcc crystals, *Acta Materialia* 85 (2015) 180–190.
- [44] T. El-Achkar, D. Weygand, Analysis of dislocation microstructure characteristics of surface grains under cyclic loading by discrete dislocation dynamics, *Modelling and Simulation in Materials Science and Engineering* 27 (2019) 055004.
- [45] A. Arsenlis, D. Parks, Crystallographic aspects of geometrically-necessary and statistically-stored dislocation density, *Acta Materialia* 47 (1999) 1597 – 1611.
- [46] A. Acharya, A model of crystal plasticity based on the theory of continuously distributed dislocations, *J. Mech. Phys. Solids* 49 (2001) 761–784.
- [47] C. Fressengeas, *Mechanics of Dislocation Fields*, Wiley-ISTE, 2017.
- [48] M. Zaiser, S. Sandfeld, Scaling properties of dislocation simulations in the similitude regime, *Modelling and Simulation in Materials Science and Engineering* 22 (2014) 0–20.
- [49] S. Haouala, S. Lucarini, J. LLorca, J. Segurado, Simulation of the hall-petch effect in fcc polycrystals by means of strain gradient crystal plasticity and fft homogenization, *Journal of the Mechanics and Physics of Solids* 134 (2020) 103755.
- [50] A. Foreman, The bowing of a dislocation segment, *Philos. Mag. A J. Theor. Exp. Appl. Phys.* 15 (1967) 1011–1021.
- [51] G. Saada, On hardening due to the recombination of dislocations, *Acta Met.* 8 (1960) 841–847.
- [52] R. Sills, N. Bertin, A. Aghaei, W. Cai, Dislocation networks and the microstructural origin of strain hardening, *Physical Review Letters* 121 (2018) 085501.

- [53] D. Hull, D. Bacon, 3 - movement of dislocations, in: D. Hull, D. Bacon (Eds.), *Introduction to Dislocations (Fourth Edition)*, fourth edition Edition, Butterworth-Heinemann, Oxford, 2001, pp. 42 – 61.
- [54] B. Devincere, L. Kubin, T. Hoc, Physical analyses of crystal plasticity by DD simulations, *Scr. Mater.* 54 (2006) 741–746.
- [55] L. Kubin, B. Devincere, T. Hoc, Modeling dislocation storage rates and mean free paths in face-centered cubic crystals, *Acta Mater.* 56 (2008) 6040–6049.
- [56] R. Madec, B. Devincere, L. Kubin, T. Hoc, D. Rodney, The role of collinear interaction in dislocation-induced hardening, *Science* 301 (2003) 1879–1882.

$\varepsilon_p = 0.1\%$  $\varepsilon_p = 0.2\%$ 